

See discussions, stats, and author profiles for this publication at: <https://www.researchgate.net/publication/231678639>

Adsorption of Gases and Vapors on Carbon Molecular Sieves

ARTICLE *in* LANGMUIR · JULY 1997

Impact Factor: 4.46 · DOI: 10.1021/la961040c

CITATIONS

79

READS

113

3 AUTHORS, INCLUDING:



Keith Mark Thomas

Newcastle University

198 PUBLICATIONS 10,403 CITATIONS

SEE PROFILE

Adsorption of Gases and Vapors on Carbon Molecular Sieves

I. P. O'koye,[†] M. Benham,[‡] and K. M. Thomas^{*,†}

Northern Carbon Research Laboratories, Department of Chemistry, Bedson Building,
University of Newcastle upon Tyne, Newcastle upon Tyne NE1 7RU, U.K., and
Hiden Analytical Ltd., 420 Europa Boulevard, Warrington, WA5 5UN, U.K.

Received October 14, 1996. In Final Form: January 21, 1997[®]

The adsorption phenomena of oxygen and nitrogen on a carbon molecular sieve were studied above the critical temperature of the adsorptives as a function of pressure in order to understand further the mechanism of air separation. The uptake of both gases studied was virtually linear at low equilibrium pressures, in agreement with Henry's law, but deviation occurred at higher pressures. The adsorption kinetics were studied with different amounts of preadsorbed gas for changes in pressure of 11 kPa and partial pressure in helium of ~10 kPa. The gas adsorption kinetics obey a linear driving force mass transfer model. The ratios of the rate constants (k_{O_2}/k_{N_2}) for each pressure increment were 35–43 for pure gases and 21–27 for gas/helium mixtures, and these ratios clearly demonstrate the molecular sieving characteristics. The presence of water vapor is detrimental to the operation of carbon molecular sieves. The adsorption and desorption characteristics of water vapor with different amounts of preadsorbed water were studied for comparison with oxygen and nitrogen adsorption over the pressure range 0–1.8 kPa for pressure steps of 0.1 kPa. The results are discussed in terms of the mechanism of gas separation using carbon molecular sieves.

Introduction

The use of carbon molecular sieves in the separation and purification of mixtures of gases with very similar molecular dimensions is of great interest in the chemical and petrochemical industries. A wide range of commercial carbon molecular sieves (CMS) have been manufactured by varying the type of precursors, method and temperature of carbonization, activation procedure, pore blocking method, and passivation techniques. These carbon molecular sieves can be prepared from coal, petroleum, biomass, and polymeric precursors^{1,2} and are used widely for gas separation³ and storage⁴ applications. A typical application is the industrial separation of air into oxygen and nitrogen by pressure swing adsorption (PSA). The capacities of this class of molecular sieves for oxygen and nitrogen adsorption are very similar, but the rates of adsorption differ considerably. The PSA technique is based on the difference between the kinetics of adsorption of oxygen and nitrogen with oxygen adsorption being much faster than nitrogen adsorption. This difference in adsorption kinetics is thought to be related to molecular size. The kinetic diameter of oxygen (0.346 nm) is slightly smaller than that of nitrogen (0.364 nm). When a carbon sample with molecular sieving characteristics comes into contact with air, an oxygen-enriched adsorbed phase and a corresponding nitrogen-rich gas phase are produced initially.

The present study involved an investigation of the kinetics of oxygen and nitrogen adsorption on a carbon molecular sieve with various amounts of preadsorbed gas for a series of pressure steps. The effects of the presence of helium gas on the adsorption kinetics and capacity of these gases were investigated. The presence of water vapor in the air is very detrimental to the performance of carbon molecular sieve materials. Therefore the

adsorption of water vapor was also investigated for comparison and to understand the mechanism by which water vapor interferes with the separation process.

Experimental Section

Materials Used. The commercial carbon molecular sieve (CMS) used in the present study was supplied by Air Products and Chemicals Inc., U.S. The CMS was prepared by carbon deposition on a microporous substrate. Helium, nitrogen, and oxygen (99.99% purity), supplied by BOC Ltd, were dried by passage through drying tubes containing activated silica gels.

Measurement of Adsorption Kinetics. The kinetic measurements were carried out using the Intelligent Gravimetric Analyser (IGA) supplied by Hiden Analytical Ltd. The IGA instrument allows the adsorption–desorption isotherms and the corresponding kinetics of adsorption or desorption at each pressure step to be determined.⁵ The system consists of a fully computerized microbalance which automatically measures the weight of the carbon sample as a function of time with the gas pressure and sample temperature under computer control. The carbon sample was outgassed to a constant weight at 383 K and 10^{-8} Pa prior to measurement of the isotherms. The pressure and temperature were then set to the desired value under computer control, and the weight uptake was measured as a function of time under isothermal conditions until equilibrium was attained. The approach to equilibrium was monitored in real time, and a computer algorithm was used to establish when 99% gas uptake was achieved. These weight versus time data were used to calculate the adsorption kinetic parameters. After equilibrium was achieved, the pressure was increased to the next desired value and the weight versus time monitored. The process was repeated until sufficient adsorption data points were obtained for the isotherm. In this technique the adsorption kinetics for a given pressure step were measured for different amounts of preadsorbed gases adsorbed at equilibrium on the carbon adsorbent. A similar procedure was used for the nitrogen/helium and oxygen/helium mixtures. In this case the partial pressure of the gas was increased in increments similar to the pure gases. The total flow rate used throughout the experiments was $100 \text{ cm}^3 \text{ min}^{-1}$. The adsorption and desorption data for water vapor were obtained in a similar manner by first increasing and then decreasing the pressure in incremental steps. Kinetic measurements were obtained for oxygen, nitrogen, and water

* Corresponding author.

[†] University of Newcastle upon Tyne.

[‡] Hiden Analytical Ltd.

[®] Abstract published in *Advance ACS Abstracts*, June 15, 1997.

(1) Metcalf, J. E.; Kawahata, M.; Walker, P. L. *Fuel* **1963**, 42, 233.

(2) Moore, S. V.; Trimm, D. L. *Carbon* **1977**, 15, 177.

(3) Sircar, S.; Golden, T. C.; Rao, M. B. *Carbon* **1996**, 34, 1.

(4) Verma, S. K.; Walker, P. L. *Carbon* **1992**, 30, 837.

(5) Benham, M. J.; Ross, D. K. Z. *Phys. Chem.* **1989**, 25, 163.

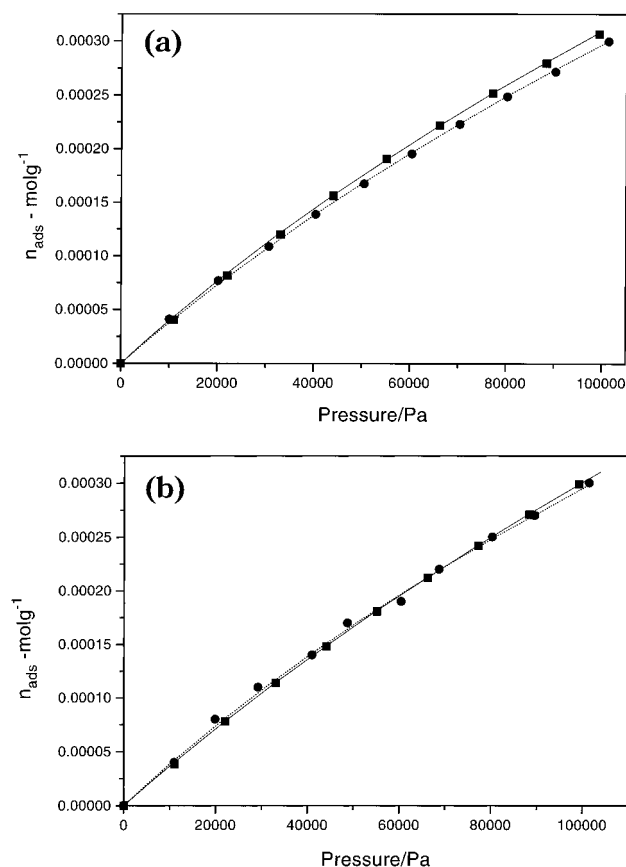


Figure 1. (a) Adsorption isotherms for nitrogen on the carbon molecular sieve; (■) N_2 , (●) N_2/He ; determined at 293 K. Isotherm fitting using virial equation parameters in Table 1; — N_2 , - - - N_2/He . (b) Adsorption isotherms for oxygen on the carbon molecular sieve; (■) O_2 , (●) O_2/He ; determined at 293 K. Isotherm fitting using virial equation parameters in Table 1; — O_2 , - - - O_2/He .

vapor at 293K only. The isotherms are typically repeatable to better than $\pm 1\%$.

Results

The carbon dioxide adsorption isotherm at 273 K for the carbon molecular sieve was Type 1. The surface area calculated from the Langmuir isotherm gave a surface area of $\sim 242 \text{ m}^2 \text{ g}^{-1}$ (based on an area of $1.7 \times 10^{-19} \text{ m}^2$ per molecule) while the micropore volume obtained by extrapolation of the Dubinin–Radushkevich equation was $0.152 \text{ cm}^3 \text{ g}^{-1}$.

Adsorption isotherms of nitrogen and oxygen at 293 K determined using the IGA are shown in Figures 1a and 1b, respectively. There is little difference in the isotherms for oxygen and nitrogen and the gases in the presence of helium. The uptakes of both gases as a function of pressure are approximately linear at low pressures, but deviations from linearity are observed as pressure increases. The adsorption temperature used in this study was above the critical temperatures of both nitrogen and oxygen, and therefore, it is not possible to express the pressures in terms of relative pressure since the saturated vapor pressure (P_0) does not exist under the aforementioned conditions. The virial plots for nitrogen and oxygen adsorption are shown in Figures 2 and 3, respectively. These graphs are linear over a major part of the pressure range but deviate at low-pressure where Henry's law is obeyed. In the low-pressure region of the adsorption isotherm, small errors produce large errors in the virial plots. Good agreement was obtained for the values of A_0 and A_1 for the adsorption of nitrogen gas and nitrogen in

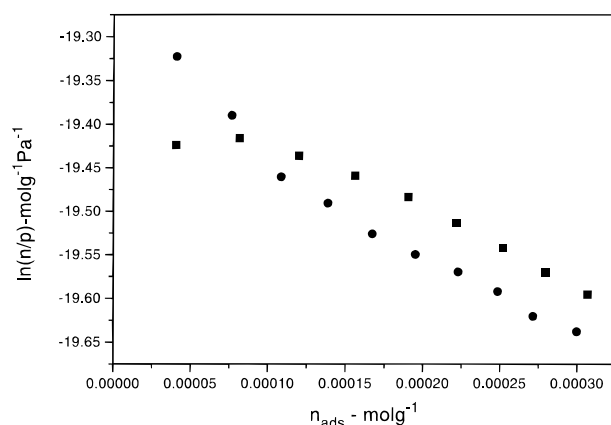


Figure 2. Virial plots for nitrogen adsorption on carbon molecular sieve at 293 K; (■) N_2 , (●) N_2/He .

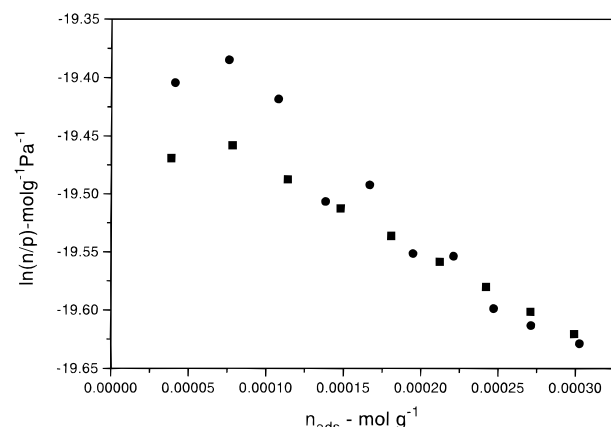


Figure 3. Virial plots for oxygen adsorption on the carbon molecular sieve at 293 K; (■) O_2 , (●) O_2/He .

Table 1. Virial Constants for Adsorption of Oxygen and Nitrogen on the CMS

	$A_1/\text{g mol}^{-1}$	$\exp(A_0) \times 10^9/\text{mol g}^{-1} \text{ Pa}^{-1}$
N_2	-921 ± 25	4.109 ± 0.002
N_2/He	-928 ± 27	3.909 ± 0.002
O_2	-736 ± 7	3.756 ± 0.001
O_2/He	-1015 ± 116	3.99 ± 0.01

helium, and the values are given in Table 1. The agreement for oxygen adsorption virial parameter was less satisfactory (see Table 1). This is due to a higher degree of scatter in the data points for oxygen/helium mixtures. The parameters obtained from the virial equation graph for nitrogen are similar to those obtained previously.⁶ The isotherms calculated from the virial coefficients for nitrogen and nitrogen/helium mixtures are shown in Figure 1a while the isotherms calculated for oxygen and oxygen/helium mixtures are shown in Figure 1b. It is apparent that in all cases there is good agreement between the isotherms calculated from the virial equation parameters and the experimentally determined isotherms. Figure 4 shows the graph of nitrogen and oxygen uptake versus time. Comparison of Figures 1 and 4 shows that the adsorption capacities for oxygen and nitrogen are very similar while the rates of adsorption differ markedly. The differences in the rate constants for the adsorption of pure gases and corresponding gas/helium mixtures for a given pressure increment are comparatively small compared to the differences in the rates of oxygen and nitrogen. Graphs of $\ln(1 - w_t/w_e)$ against time t where w_t and w_e

(6) Cole, J. H.; Everett, D. H.; Marshall, C. T.; Paniego, A. R.; Powl, J. C.; Rodriguez-Reinoso, F. *J. Chem. Soc., Faraday Trans. 1* **1974**, 70, 2154.

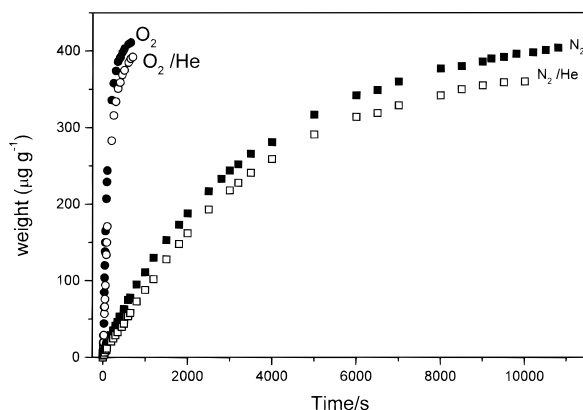


Figure 4. Variation of the gas uptake with time for the adsorption of nitrogen and oxygen on the carbon molecular sieve at 293 K. Pressure ranges: (a) pure gases, 55–66 kPa; (b) gas/helium mixtures, N₂ 40.3–50.2 kPa, O₂ 41.2–48.9 kPa.

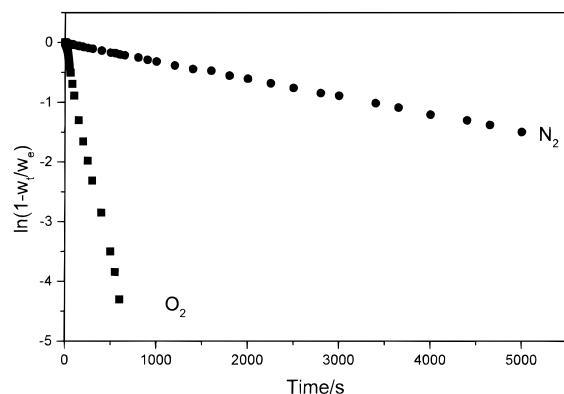


Figure 5. Variation of $\ln(1 - w_t/w_e)$ against time for the adsorption of N₂ and O₂ on the carbon molecular sieve at 293 K. Pressure range: 55–66 kPa.

refer to the adsorbate weight uptake at time t and at equilibrium, respectively, for the uptake of both gases at 293 K are shown in Figure 5. It is apparent that the gas uptakes for both oxygen and nitrogen on this class of molecular sieve follow a linear driving force mass transfer kinetic model already discussed elsewhere,⁷ where $w_t/w_e = 1 - e^{-kt}$, with linear graphs of $\ln(1 - w_t/w_e)$ against time. The rate of nitrogen and oxygen uptake can be compared in terms of the pseudo-first-order rate constant, k , which is determined from the gradient of the kinetic plot as shown in Figure 5. The full kinetic data presented in Table 2 indicate that the rate of uptake of nitrogen is much slower and involves longer equilibrium times compared with that of oxygen. Comparison of the rate constants for gases and the gas mixtures in helium is complicated by the slightly different pressure increments. However, the rate constants for both nitrogen and oxygen adsorption for a given pressure increment increase slightly with increasing initial pressure both for pure gases and for mixtures with helium. The kinetic selectivity for the carbon molecular sieves can be obtained from the ratio of the rate constants for nitrogen and oxygen (see Table 2). It is apparent that the ratio decreases with increasing pressure.

Figure 6 shows the adsorption–desorption isotherm of water determined at 293 K. It is evident that the water isotherm is Type V and remarkably different from that of nitrogen or oxygen. This is due to the different mechanism of adsorption which involves initial adsorption on primary

Table 2. Kinetic Data for Nitrogen and Oxygen Gas Adsorption on Carbon Molecular Sieve Determined at 293 K^a

(a) Pure Gases				
pressure (kPa)	pure N ₂ (k/s × 10 ⁻⁴)	pure O ₂ (k/s × 10 ⁻⁴)	kO ₂ /kN ₂	
0–11	2.143 ± 0.011	83.5 ± 0.7	39.0	
11–22	2.20 ± 0.01	88.9 ± 0.9	40.4	
22–33	2.325 ± 0.009	99.5 ± 1.0	42.8	
33–44	2.452 ± 0.014	99.6 ± 1.1	40.6	
44–55	2.612 ± 0.011	104.1 ± 1.2	39.9	
55–66	2.824 ± 0.013	105.1 ± 1.3	37.2	
66–77	2.971 ± 0.014	109.3 ± 1.4	36.8	
77–88	3.134 ± 0.016	111.3 ± 1.5	35.5	
88–99	3.226 ± 0.017	113.9 ± 1.6	35.3	
(b) Gas Mixtures				
partial pressure N ₂ (kPa)	N ₂ /He (k/s × 10 ⁻⁴)	partial pressure O ₂ (kPa)	O ₂ /He (k/s × 10 ⁻⁴)	kO ₂ /kN ₂
0.5–10.5	2.662 ± 0.022	0.4–11.4	58.2 ± 0.5	21.9
10.5–20.4	2.313 ± 0.011	11.4–20.2	62.7 ± 0.4	27.1
20.4–30.8	2.444 ± 0.013	20.2–29.6	65.3 ± 0.4	26.7
30.8–40.3	2.572 ± 0.011	29.6–41.2	67.8 ± 0.4	26.4
40.3–50.2	2.721 ± 0.019	41.2–48.9	69.9 ± 0.4	25.7
50.2–59.9	2.848 ± 0.014	48.9–60.5	70.1 ± 0.5	24.6
59.9–69.7	2.824 ± 0.016	60.5–68.8	72.1 ± 0.5	25.5
69.7–79.4	2.907 ± 0.018	68.8–80.3	73.0 ± 0.5	25.1
79.4–89.1	3.050 ± 0.023	80.3–89.4	74.7 ± 0.5	24.5
89.1–100.1	3.407 ± 0.019	89.4–101.2	71.9 ± 0.4	21.1

^a Error bars obtained from the kinetic graphs.

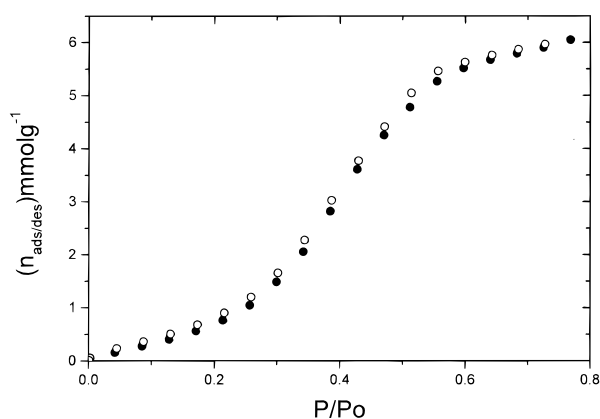


Figure 6. Adsorption–desorption isotherms of water on the carbon molecular sieve at 293 K; (●) adsorption, (○) desorption.

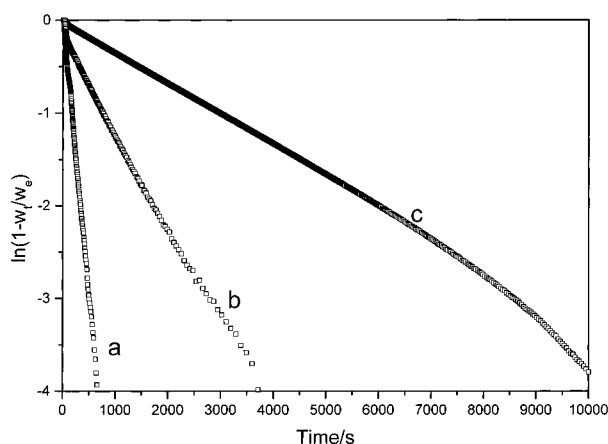
centers followed by the growth of clusters of water molecules around these centers. The adsorption–desorption hysteresis is small in these carbon molecular sieves, which is in contrast to adsorption on activated carbons which have a wider pore size distribution.⁸ In addition, the steep increase in water vapor uptake around p/p_0 0.3–0.4 is lower than for active carbons (p/p_0 0.45–0.65) which have a wider pore size distribution. Figure 7 shows graphs of $\ln(1 - w_t/w_e)$ versus time for water vapor uptake for pressure steps of (a) 0–100 Pa, (b) 1617–1718 Pa, and (c) 911–1012 Pa. It is apparent that the graphs are straight lines for >90% of the uptake. This confirms that the adsorption kinetics follow a linear driving force mass transfer model for the pressures steps used. The results also show that the rate constants differ markedly for the different pressure increments. Figure 8 shows a graph of rate constant versus water vapor pressure. This graph shows three distinct regions corresponding to specific processes in the water adsorption mechanism. The initial

(7) Chagger, H. K.; Ndaji, F. E.; Sykes, M. L.; Thomas, K. M. *Carbon* **1995**, 33, 1411.

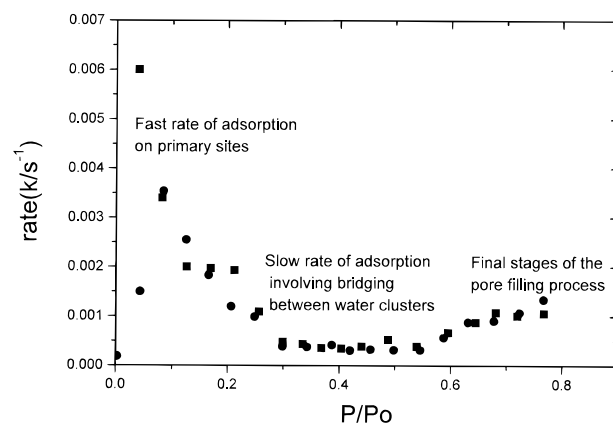
(8) Foley, N. J.; Forshaw, P. L.; Thomas, K. M.; Stanton, D.; Norman, P. R. *Langmuir* **1997**, 13, 2083.

Table 3. Kinetic Data for Water Adsorption on the Carbon Molecular Sieve at 293 K

pressure range (Pa)	adsorption		pressure range (Pa)	desorption	
	capacity ^a (mmol g ⁻¹)	rate constant (s ⁻¹ × 10 ⁻⁴)		capacity ^a (mmol g ⁻¹)	rate constant (s ⁻¹ × 10 ⁻⁴)
0–100	0.158	59.98 ± 0.02	106–1	0.235	15.29 ± 0.01
100–202	0.277	33.85 ± 0.01	207–106	0.363	35.42 ± 0.02
202–304	0.405	19.78 ± 0.02	309–207	0.505	25.45 ± 0.01
304–404	0.562	19.70 ± 0.01	410–309	0.679	18.55 ± 0.01
404–506	0.766	19.30 ± 0.01	511–410	0.903	12.11 ± 0.01
506–607	1.05	10.89 ± 0.02	613–511	1.20	10.12 ± 0.03
607–709	1.49	4.86 ± 0.01	714–613	1.66	3.92 ± 0.03
709–809	2.06	4.41 ± 0.01	815–714	2.28	3.84 ± 0.01
809–911	2.82	3.57 ± 0.01	916–815	3.03	4.20 ± 0.01
911–1012	3.61	3.53 ± 0.01	1017–916	3.77	3.13 ± 0.03
1012–1114	4.26	3.93 ± 0.01	1116–1017	4.42	3.42 ± 0.04
1114–1212	4.78	3.25 ± 0.03	1217–1116	5.05	3.39 ± 0.01
1212–1314	5.27	3.88 ± 0.01	1319–1217	5.46	3.25 ± 0.01
1314–1414	5.52	6.73 ± 0.01	1420–1319	5.63	5.78 ± 0.04
1414–1515	5.67	8.76 ± 0.02	1521–1420	5.76	8.80 ± 0.03
1515–1617	5.79	10.96 ± 0.03	1622–1521	5.87	9.08 ± 0.01
1617–1718	5.90	10.08 ± 0.04	1723–1622	5.97	11.03 ± 0.01
1718–1820	6.05	10.59 ± 0.03	1820–1723	6.05	13.76 ± 0.01

^a Refers to higher pressure in range.**Figure 7.** Variation of water vapor uptake with time on the carbon molecular sieve at 293 K. Pressure ranges: (a) 0–100 Pa; (b) 1617–1718 Pa; (c) 911–1012 Pa.

stage indicates a fast rate constant of adsorption on primary sites, while the slowest rate constant occurs at intermediate pressure range and this corresponds to the growth of clusters of water molecules around the primary centers within the pressure range of 0.7–1.2 kPa leading to bridging between pore walls and pore filling. The increase in rate constant at high vapor pressures > 1.2 kPa corresponds to the final stages of pore filling. The reverse applies for the desorption of water molecules from the carbon molecular sieve. The adsorption and desorption parameters for water vapor on the carbon molecular sieve are given in Table 3. It is apparent from these data that the adsorption–desorption hysteresis is small while the rates constants for adsorption and desorption are very similar over a given pressure range. The similarity between the adsorption and desorption rate constants was observed previously for active carbons where the adsorption/desorption isotherms showed significant hysteresis.⁸ The total water uptake at p/p_0 0.76 was 6.05 mmol g⁻¹ which corresponds to a pore volume of 0.109 cm³ g⁻¹. The shape of the water adsorption isotherm indicates that higher relative humidities will not lead to greatly enhanced adsorption of water. The presence of the hydrophobic surfaces and the ultra-microporous structure of the carbon molecular sieve produces an adsorbed phase which has a lower density than water. This needs to be considered in the calculation of pore volumes using water adsorption

**Figure 8.** Variation of rate constant for water adsorption–desorption on the carbon molecular sieve as a function of vapor pressure at 293 K; (■) adsorption, (●) desorption.

data, and the pore volume calculation needs to be taken in this context.

Discussion

Generally, little attention has been paid to the adsorption of gases by solids at temperatures well above the critical temperature of the adsorptives. So far most studies in the literature have been carried out at temperatures well below the gas critical temperature where the amounts adsorbed are much higher and the pressures under which adsorption takes place can be compared relative to the saturated vapor pressures.⁹ Above the critical temperature theoretical interpretation of the results is possible in terms of nonideal gas theory but comparisons of various gases are difficult. However, it is well established that at sufficiently low coverage, adsorption occurs via adsorbate–solid interactions with the exclusion of pairwise interactions between the adsorbed molecules. The exclusion of this latter phenomenon ensures that Henry's law is obeyed reasonably. Thus at low surface coverages the adsorption obeys the equation $n = K_H p$, where n is the amount adsorbed per unit mass of adsorbent at equilibrium pressure p and K_H is Henry's law constant. The Langmuir theory degenerates to a mere empiricism, and the calculation and meaning of the saturation uptake

(9) Rodriguez-Reinoso, F. R.; Garrido, J.; Martin-Martinez, J. M.; Molina-Sabio, M.; Torregrosa, R. *Carbon* **1989**, 27, 23.

(monolayer coverage) under this condition become completely erroneous and difficult to interpret. As a result, a pseudo or apparent monolayer instead of a true value is obtained from the linear graph of p/n versus p . Nicholson and Sing¹⁰ analyzed adsorption data using a virial equation and reported that at very low pressures virial expansions reduce to Henry's law. The virial equation can be written in two forms:⁶

$$n/p = K_0 + K_1p + K_2p^2 + \dots \quad (1)$$

$$\ln(n/p) = A_0 + A_1n + A_2n^2 + \dots \quad (2)$$

where n is the amount adsorbed at pressure p and the first coefficient of the two equations are related by

$$K_0 = \exp(A_0) = \text{Henry's Law constant} \quad (3)$$

The term K_0 is equal to the Henry's law constant and totally dependent on the interaction between the adsorbent surfaces and the adsorbed gas molecules. Under the conditions of the present study, low pressure and low surface coverage, it is meaningless to extend the analysis beyond the first and second terms in eq 2. Furthermore, higher terms in eqs 1 and 2 are only important at much higher pressures. The values of A_0 can be obtained from the graphs of $\ln(n/p)$ versus n at a series of temperatures T . Also from the slope of the plot of $\ln K_0$ against $1/T$, the limiting isosteric heat of adsorption can be estimated. Cole et al. investigated⁶ the adsorption of nitrogen, krypton, and xenon on various carbons over the temperature range 273–398 K. The values of $\exp(A_0)$ and the A_1 values for nitrogen adsorption were in the range from 1.18×10^{-9} to $7.55 \times 10^{-9} \text{ mol g}^{-1} \text{ Pa}^{-1}$ and from 89 to 640 g mol^{-1} , respectively. Comparison of these values for $\exp(A_0)$ and A_1 with the values obtained in this study at 293 K shows that they are similar. Studies of the adsorption of oxygen and nitrogen on another sample from the same batch of CMS over the pressure range 0–0.9 MPa gave virial equation graphs similar to those in Figures 3 and 4.¹¹ The graphs had excellent linearity and A_1 values in the range -674 ± 5 and $-966 \pm 5 \text{ g mol}^{-1}$ for oxygen and nitrogen, respectively. The results also showed that the kinetics followed a linear mass transfer kinetic model over the whole pressure range and that the rate constants for adsorption increase with increasing pressure over the pressure range 0–0.9 MPa for pressure steps of 0.1 MPa.

The carbon molecular sieve under study has a bimodal pore size distribution with a narrow micropore size range. Adsorption will occur at low relative pressures in the ultra-micropores, which are the more energetic sites.^{12–14} The kinetic results in Figures 4 and 5 and in Table 1 show clearly the more rapid kinetics for oxygen adsorption compared with nitrogen, but both gases have similar adsorption capacities. Previous adsorption kinetic studies show that oxygen can penetrate the carbon pore structure more rapidly than nitrogen.^{7,15,16} This is related to the molecular size of the oxygen which is slightly smaller than

the critical pore dimension responsible for the selectivity of the carbon molecular sieve. In contrast the molecular dimension of nitrogen is slightly larger than oxygen, thus there is a larger barrier for diffusion into the porous structure.

The adsorption rate constants for N_2 and N_2 in He are virtually identical within experimental error. However, the adsorption rate constant for O_2 is significantly higher than that for O_2 in helium. This suggests that, in the case where the rates of adsorption are fast, bulk diffusion in the pores is a factor that influences the rate of adsorption.

Rao et al.¹⁷ have carried out mathematical modeling studies of the diffusive potentials within carbon molecular sieves. The model was based on that developed by Steele¹⁸ for the interaction of gases with solid surfaces and involved the summation of the atom–atom interactions over the entire solid. The interaction was described by a Lennard-Jones function with parameters derived from the Lorentz–Berthelot combining rules. The approach allowed the diffusion of gases to be characterized along the pore centerline of slit-shaped pores whose walls were composed of basal planes. They concluded that two barriers existed, (1) entering the pore and (2) diffusion along the pore, and that the rate-limiting process was entry through the pore aperture. The calculations predicted that nitrogen and carbon dioxide diffused at similar rates in the pores. The energy barrier for pore entry for carbon dioxide was zero whereas for nitrogen it was $\sim 24 \text{ kJ mol}^{-1}$, indicating that the entry into the pore was the rate-limiting process. Previous studies⁷ of the adsorption of oxygen and nitrogen at atmospheric pressure on CMS similar to the one used in this study over the temperature range 275–333 K have shown differences in the pre-exponential factors and activation energies. The activation for nitrogen adsorption was 34.6 kJ mol^{-1} , while the corresponding value for oxygen was 30.9 kJ mol^{-1} . The pre-exponential factor for nitrogen was 650 s^{-1} whereas the corresponding value for oxygen was 3500 s^{-1} . The activation energy for the diffusion of carbon dioxide into the carbon molecular sieve was much lower, $\sim 12 \text{ kJ mol}^{-1}$. These results show similar trends to the theoretical studies. The carbon molecular sieve used in this study was prepared by carbon deposition. In this type of material, the carbon deposition on the nonselective substrate is heterogeneous and as a consequence reduction in the particle size results in the gradual reduction of the molecular sieving characteristics due to the production of nonselective pathways for gas adsorption.⁷

Adsorption and desorption isotherms for water vapor on the CMS (see Figure 6) are given in terms of the amount adsorbed versus relative pressure, p/p_0 , here p_0 is the saturated vapor pressure of water. The isotherm for water vapor was type V.¹⁹ It is apparent from Figure 8 that the adsorption and desorption rate constants determined from water vapor adsorption on the carbon molecular sieve were smaller than those of oxygen and similar to nitrogen while the amounts adsorbed were much larger even though the vapor pressures were low compared with the gas pressures. The transport of water molecules into the carbon molecular sieve is different from oxygen and nitrogen, and this may be due to the following reasons: (1) the planar shape of the water molecule which will affect transport through the selective porosity and (2) the adsorption mechanism which is different from that of both oxygen and nitrogen. The water adsorption isotherm and kinetics are similar

(10) Nicholson, D.; Sing, K. S. W. *Colloid Science*; Everett, D. H., Ed.; Chemical Society: London, 1979; Vol. 3, pp 1–62.

(11) I. P. O'Koye and K. M. Thomas unpublished results.

(12) Carrott, P. J. M.; Roberts, R. A.; Sing, K. S. W. *Carbon* **1987**, 25, 59.

(13) Dubinin, M. M. In *Characterisation of Porous Solids*; Gregg, S. J., Sing, K. S. W., Stoeckli, H. F., Eds.; Society of Chemical Industries: London, 1979; pp 1–11.

(14) Dubinin, M. M.; Astakhov, V. A. *Adv. Chem. Ser.* **1971**, 102, 69; *J. Colloid Interface Sci.* **1980**, 75, 34.

(15) Koresh, J.; Soffer, J. J. *J. Chem. Soc., Faraday Trans. 1* **1980**, 76, 2472.

(16) Nandi, S. P.; Walker, P. L. *Fuel* **1975**, 54, 169.

(17) Rao, M. B.; Jenkins, R. G.; Steele, W. A. *Ext. Abstr. Program—Biennial Conf. Carbon 17th*, **1985**, 114.

(18) Steele, W. A. *Surf. Sci.* **1973**, 36, 317.

(19) Gregg, S. J.; Sing, K. S. W., Eds. *Adsorption, Surface Area, and Porosity* 2nd ed.; Academic Press: New York, 1982.

to those observed previously for an active carbon.⁸ Also the CMS has a relatively high uptake of water vapor. These observations suggest that molecular sieving effects are of limited significance for water vapor adsorption in this case. The adsorption kinetics were found to occur in three stages over the pressure range starting with a very fast uptake at the initial stage occurring on the primary adsorption sites in the carbon micropore structure. As shown in Figure 8, in the low-pressure region, fast adsorption occurs at low surface coverage on primary adsorption sites, for example, oxygen functionality in the carbon structure. Water molecules are thought to adsorb not only on the available empty sites but also on adsorbed water molecules forming groups of clusters around the primary sites. In the intermediate stage it was proposed that these groups of clusters will eventually connect, bridging between pore walls which effectively approach pore filling at sufficiently high pressures.²⁰ At higher relative pressures, some cooperative effects are apparent. The adsorption of water vapor in significant quantities will lead to the filling of available porosity and this adsorbed water will be difficult to desorb due to the slow kinetics for the major part of the adsorbed water uptake. It has not been possible to measure oxygen and nitrogen adsorption in the presence of water vapor due to the much lower quantities of oxygen and nitrogen adsorbed compared with water vapor. In view of rates of adsorption-desorption being slowest in the pressure range where changes in adsorption capacity are greatest, it is likely that the detrimental effect of water vapor on molecular sieving is related to water vapor kinetics and blocking of available porosity.

The amount of water vapor adsorbed at p/p_0 0.76 was equivalent to a pore volume of $0.109 \text{ cm}^3 \text{ g}^{-1}$, while the micropore volume obtained from the Dubinin-Radushkevich graph was $0.152 \text{ cm}^3 \text{ g}^{-1}$. The shape of the water vapor adsorption isotherm suggests that the capacity will not increase greatly with further increase in vapor pressure. The observation that the pore volume determined from water vapor adsorption was usually lower than the total pore volume obtained from nitrogen adsorption has been reported previously.^{8,21-23} Values for the ratio have ranged from 0.22 to 0.9. In the case of a carbon with a low extent of activation a value greater than 1 was obtained, and this was ascribed to activated diffusion effects leading to an anomalously low pore volume calculated from nitrogen adsorption at 77 K. In the case of adsorption of CMS materials the total pore volume cannot be obtained from nitrogen adsorption at 77 K because of activated diffusion effects and the micropore volume determined from CO_2 adsorption data is used for comparison. The ratio of the water vapor uptake to the micropore volume was 0.72. Previous studies by Bradley *et al.*²² observed low values (0.22 and 0.28) for the ratio of the pore volume estimated from water vapor adsorption at p/p_0 0.9 to total pore volume obtained from nitrogen

adsorption for two commercially available active carbons. However, other studies^{8,21,23} have reported values in the range 0.7–0.8 for the ratio which are similar to the results obtained for the carbon molecular sieve.

The reason for the lower pore volume determined from water vapor adsorption may be explained by differences in the structure of adsorbed water compared with water. The reason for this is possibly related to the water molecules associated with primary adsorption centers and adjacent to hydrophobic surfaces have different structures to water. Carrot *et al.* have proposed that the low ratio of water vapor uptake compared to nitrogen adsorption for Silicalite was due to the inability of water to form a three-dimensional hydrogen-bonded structure in the cylindrical micropores which have a diameter of $<500 \text{ pm}$.²⁴ Foley *et al.* have shown⁸ that for a carbon composed of mainly ultra-microporosity with a sharp decrease in capacity in the 400–460 nm range that the ratio of the pore volumes determined from water vapor and nitrogen adsorption at 77 K was 0.78.⁸ The carbon molecular sieve used in this study was prepared by carbon deposition on a microporous substrate and has a similar micropore size distribution to the active carbon but shifted to slightly lower pore sizes. However, this is an apparent micropore size distribution because grinding the sample results in loss of molecular sieving characteristics due to the introduction of nonselective adsorption pathways.⁷ It is evident that the proposal involving the inability of adsorbed water to form a three-dimensional network structure in ultra-microporosity is a possible explanation of the relatively low water vapor adsorption capacity compared to the micropore volume.

Conclusions

The adsorption characteristics of oxygen and nitrogen on the carbon molecular sieve material are substantially different from water vapor. The rate constants for oxygen and nitrogen adsorption on the CMS differ by a factor of ~ 20 , indicating a kinetic rather than thermodynamic effect. The rates of adsorption for oxygen and nitrogen increase slightly with increasing amounts of initial preadsorbed gas for a given pressure increment both for the pure gases and for the gas/helium mixtures. The adsorption of water vapor is detrimental to the performance of carbon molecular sieves. The rates of water vapor adsorption-desorption vary considerably with the vapor pressure, and this is related to the adsorption-desorption mechanism. These rates of adsorption-desorption are slowest in the pressure range where changes in water adsorption capacity are at a maximum. Therefore it is likely that the detrimental effect of the water vapor is related to this and the blocking of the available porosity in the carbon molecular sieve by the adsorbed water. The water vapor will occupy adsorption sites on the carbon even at relatively low vapor pressures.

LA961040C

(20) Muller, E. A.; Rull, L. F.; Vega, L. F.; Gubbins, K. E. *J. Phys. Chem.* **1996**, *100*, 1189.

(21) Arnell, J. C.; McDermott, H. L. *Can. J. Chem.* **1952**, *30*, 177.

(22) Bradley, R. H.; Rand, B. *Carbon* **1991**, *29*, 1165.

(23) Freeman, J. J.; Tomlinson, J. B.; Sing, K. S. W.; Theocharis, C. R. *Carbon* **1993**, *31*, 865.

(24) Carrot, P. J. M.; Kenny, M. B.; Roberts, R. A.; Sing, K. S. W.; Theocharis, C. R. In *Characterisation of Porous Solids*; Rodriguez-Reinoso, F.; Rouquerol, J.; Sing, K. S. W., Unger, K. K., Eds.; Elsevier: Amsterdam, 1991; Vol. 2, pp 685–692.